Brain Stimulation 18 (2025) 1566–1578

Contents lists available at ScienceDirect

Brain Stimulation

journal homepage: www.journals.elsevier.com/brain-stimulation

Dual-site beta transcranial alternating current stimulation during a bimanual coordination task modulates functional connectivity between motor areas

Mareike A. Gann [a,b], Ilenia Paparella [b,c], Catharina Zich [b,d,e], Ioana-Florentina Grigoras [b,e], Silvana Huertas-Penen [f], Sebastian W. Rieger [b,g], Axel Thielscher [h,i], Andrew Sharott [e], Charlotte J. Stagg [b,e,1], Bettina C. Schwab [a,f,*,1]

[a] Department of Neurophysiology and Pathophysiology, University Medical Center Hamburg-Eppendorf, Hamburg, Germany
[b] Wellcome Centre for Integrative Neuroimaging, FMRIB, Nuffield Department of Clinical Neurosciences, University of Oxford, Oxford, UK
[c] GIGA-Research, Cyclotron Research Center-In Vivo Human Imaging Unit, University of Liège, Liège, Belgium
[d] Department for Clinical and Movement Neuroscience, UCL Queen Square Institute of Neurology, University College London, London, UK
[e] Medical Research Council Brain Network Dynamics Unit, Nuffield Department of Clinical Neurosciences, University of Oxford, Oxford, UK
[f] Biomedical Signals and Systems, Electrical Engineering, Mathematics and Computer Science, University of Twente, Enschede, the Netherlands
[g] Wellcome Centre for Integrative Neuroimaging, Oxford Centre for Human Brain Activity, Department of Psychiatry, University of Oxford, Oxford, UK
[h] Section for Magnetic Resonance, DTU Health Tech, Technical University of Denmark, Kgs Lyngby, Denmark
[i] Danish Research Centre for Magnetic Resonance, Department of Radiology and Nuclear Medicine, Copenhagen University Hospital - Amager and Hvidovre, Copenhagen, Denmark

ARTICLE INFO

Keywords:
Transcranial alternating current stimulation
Functional connectivity
Bimanual coordination
Primary motor cortex
Supplementary motor cortex
Premotor cortex
Interhemispheric connectivity

ABSTRACT

Background: Communication within brain networks depends on functional connectivity. One promising approach to modulate such connectivity between cortical areas is dual-site transcranial alternating current stimulation (tACS), which non-invasively applies weak alternating currents to two brain areas.
Objectives: In the current study, we aimed to modulate inter-regional functional connectivity with dual-site tACS to bilateral primary motor cortices (M1s) during bimanual coordination and, in turn, alter behaviour.
Methods: Using functional magnetic resonance imaging (fMRI), we recorded participants' brain responses during a bimanual coordination task in a concurrent tACS-fMRI design. While performing a slow and fast version of the task, participants received one of three types of beta (20 Hz) dual-site tACS over both M1s: zero-phase, jittered-phase or sham, in a within-participant, repeated measures design.
Results: While we did not observe any significant tACS effects on behaviour, the study revealed an attenuation effect of zero-phase tACS on interhemispheric connectivity. Additionally, the two active types of tACS (zero-phase and jittered-phase) differed in the task-related M1 connectivity with other motor cortical regions, such as premotor cortex and supplementary motor area. Furthermore, individual E-field strengths were related to functional connectivity in the zero-phase condition.
Conclusions: Dual-site beta tACS over both M1s altered functional connectivity between motor areas. However, this effect did not translate significantly to the behavioural level in the presence of a restricted sample size. Future studies may thus integrate mechanistic measures, such as measures of interhemispheric inhibition, to strengthen causal interpretations.

1. Introduction

Communication within networks of anatomically distinct brain regions is crucial for supporting human cognition across the breadth of behaviours [1,2]. Communication within these networks depends on structural and functional connections between different brain regions in

* Corresponding author.Biomedical Signals and Systems Technical Medical Centre University of Twente, the Netherlands
E-mail address: b.c.schwab@utwente.nl (B.C. Schwab).
[1] These authors share senior authorship.

https://doi.org/10.1016/j.brs.2025.08.011
Received 6 April 2025; Received in revised form 25 July 2025; Accepted 18 August 2025
Available online 19 August 2025

the network. Functional connectivity (FC) can be shaped on a short time scale and therefore provides an essential addition to structural connectivity to support relatively rapid neuroplastic changes. For example, FC in motor networks has been linked to bimanual coordination [3–7], with stronger interhemispheric coupling between the primary sensorimotor cortices - specifically in the beta band - relating to better behavioural performance [3]. Understanding and modulating these coupling mechanisms through changes in functional connectivity opens new opportunities to target pathological networks in clinical settings, for example in Parkinson's disease or after stroke.

Yet, although many studies have investigated the correlation between FC and behaviour across a range of functional domains, the degree to which FC between brain regions *causally* underpins the correlated behaviour is still unclear. To determine causality, interventions which specifically modulate FC are required. One promising approach to modulate FC between cortical areas is transcranial alternating current stimulation (tACS), a form of non-invasive brain stimulation (NIBS), that applies weak alternating currents to the scalp to entrain neural responses [8–11].

A recent tACS study [12] showed that beta (20 Hz) tACS over the left primary motor cortex (M1) modulated the pattern of FC within the motor network, as observed with functional magnetic resonance imaging (fMRI) during rest. However, multiple questions remain to understand how tACS is able to modulate motor FC. Firstly, it is likely that tACS interacts with networks differently depending on how engaged they are in performing a task (so-called state-dependency, [13–15]). To simultaneously observe brain responses and apply tACS during a motor task, fMRI is the method of choice, given that, compared to electroencephalography (EEG) or magnetoencephalography (MEG) there are no problematic tACS-induced artefacts [16]. Nevertheless, very few studies have directly investigated the effects of tACS on active motor networks with fMRI. Secondly, applying tACS at two different sites opens the possibility to compare the different phase shifts of the applied currents and to potentially selectively modulate FC between the two sites. However, tACS has not often been used to modulate brain responses in more than one node within the motor network. Finally, tACS is typically used at an intensity of 2 mA peak-to-peak or lower [17]. tACS applied at higher current amplitudes is thought to entrain ongoing neural oscillation towards the externally applied frequencies more effectively than lower currents [17–19], potentially offering a more robust method to modulate FC.

Here, we aimed at investigating the role of communication in the beta band in inter-regional FC within the motor network. We did this in the context of a bimanual coordination task that requires meaningful communication between the two M1s. Bimanual coordination (i.e., the interplay of both hands) relies on interhemispheric FC within the beta band (13–30 Hz) between several motor areas [3,4,6]. This process not only underlies tasks used in the laboratory, such as finger tapping, cycling finger movements and extension/flexion of fingers and hands - but also everyday activities, such as typing or knitting. Indeed, motor beta interhemispheric FC can be disrupted in healthy aging as well as in neurological conditions such as stroke or Parkinson's disease [20–23] and modulating beta functional connectivity using dual-site tACS is therefore a highly promising target for rehabilitative therapies to improve everyday bimanual coordination. Thus, we wanted to determine whether tACS interacts with a network differentially depending on how active that network is. To do this, we used a bimanual task requiring two levels of engagement, elicited by slow and fast movements.

Specifically, we used high-definition dual-site, zero-phase, 20 Hz tACS over both M1s at a 4 mA peak-to-peak amplitude, which is thought to entrain FC between both homologous areas to the stimulation frequency and consequently strengthen FC [24–26]. However, it is still unclear how zero-phase dual-site tACS interacts with ongoing task-related oscillations. Nevertheless, strengthened FC, in turn, should lead to improved behavioural performance. We also investigated a dual-site tACS protocol with a changing phase-relationship between both hemispheres (jittered-phase tACS) at the same intensity, which is thought to lead to similar sensations but different modulations of interhemispheric FC [24]. In the context of bimanual coordination, we expected such jittered-phase beta dual-site tACS to attenuate FC and consequently decrease task performance. Specifically, to investigate task-related FC we analysed psychophysiological interactions of task-relevant regions on the primary motor cortex.

Altogether, in this fMRI study we employed focalised tACS on the two most important nodes of the active motor network to modulate and read out inter-regional FC as well as the associated bimanual coordination behaviour at varying task demands.

2. Methods

2.1. Participants

Twenty-four volunteers provided written informed consent to participate in accordance with the Central University Research Ethics Committee approval (University of Oxford; CUREC ethics reference R68812). All participants were eligible for tACS and MRI, reported no current psychiatric or neurological disorders, and had normal or corrected-to-normal vision. Six volunteers withdrew during the study due to timing constraints (N = 1, withdrawal after visit 1), non-compliance with instructions (N = 1, exclusion during the start of visit 2), or feeling uncomfortable during tACS application (N = 1 withdrew during the tACS familiarisation of visit 1, N = 1 withdrew after visit 1, N = 2 withdrew during the tACS familiarisation of visit 2 outside the MR scanner) and were not included in any analysis. Eighteen young healthy right-handed participants completed both sessions of the current study (age 24.11 ± 3.28 years, range 20–31 years; 10 females; see Supplementary Fig. S1). Of these eighteen participants, one participant was subsequently identified as an outlier in behaviour (>3 standard deviations above the coordination values of the rest of the sample) and was therefore excluded. One other volunteer only completed two of the three task runs due to technical difficulties in the zero-phase condition task run. Therefore, the analyses included data from 17 or 16 (for fMRI analyses including the zero-phase condition) volunteers. All participants received financial compensation for their participation.

2.2. Experimental design

Volunteers participated in two experimental visits (at least one week apart; 15.61 ± 9.53 days between the two visits). During the first visit, participants were familiarised with tACS (as applied with two round rubber electrodes of 40 mm diameter on EEG locations F4 and PO4) and the bimanual coordination task. They also completed two runs of the bimanual coordination task to ensure that they understood the task demands.

During the second visit, the volunteers were familiarised with the tACS setup as used inside the MRI scanner and practiced the bimanual coordination task again outside the MRI scanner. Inside the MR scanner, volunteers performed three task runs (of 16 task blocks each) with concurrent tACS of approximately 13 min each. Task scans were interleaved with T1-and T2-weighted structural scans (Fig. 1A). After each concurrent tACS-task run, volunteers were asked about the strength of the sensations that they felt due to the brain stimulation from 1 = absent to 5 = strong. After the MRI scans, volunteers filled in an extensive questionnaire on sensations during tACS (see Supplementary Fig. S2 and Supplementary Results).

2.3. Bimanual coordination task

Participants performed asymmetrical alternating movements using MR-compatible grip force sensors (Grip Force Bimanual Fiber Optic Response Pad, HHSC-2x1-GRFC-V2, Current Designs Inc., Philadelphia,

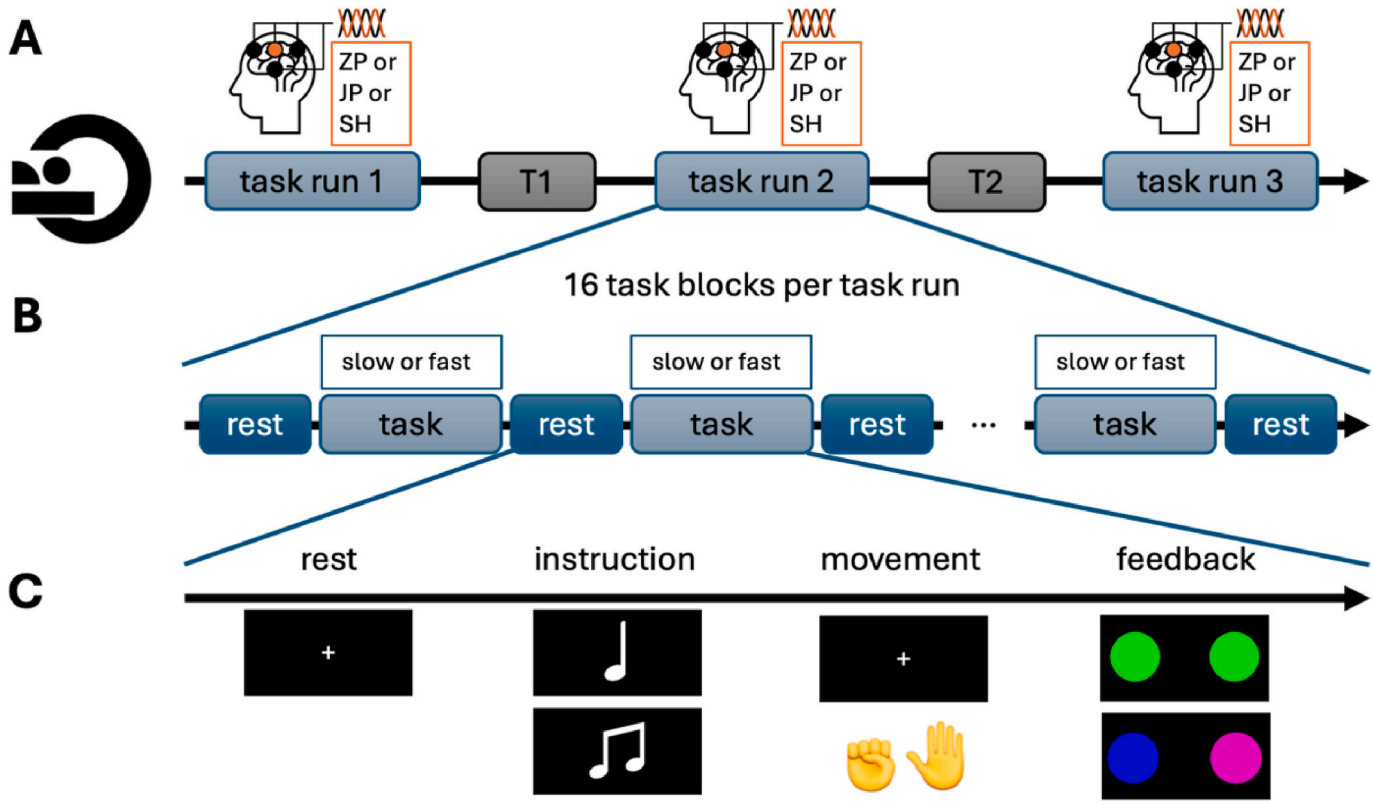

Fig. 1. Overview of the MR and task setup. (A) The MR part of the study during visit 2 consisted of three task runs with concurrent tACS and two structural scans (T1 and T2 for T1-and T2-weighted data, respectively). (B) Each task run consisted of 16 task blocks, alternating between slow and fast task blocks, interleaved with rest blocks. (C) Each task block following a 15 s rest block started with a 2 s instruction screen, then the volunteers performed the alternating movements in sync with the presented metronome sound for 30 s and saw feedback on the applied force for 1 s. MR – magnetic resonance, tACS – transcranial alternating current stimulation, ZP – zero-phase tACS, JP – jittered-phase tACS, SH – sham tACS.

PA, United States) synchronized to metronome sounds, presented at 3.8 Hz for the slow and 6 Hz for the fast task blocks. Participants were required to make smooth, well-coordinated alternating hand movements, with each hand squeezing the force grip sensors in sync with a metronome sound. The task was implemented in MATLAB R2016b (The MathWorks Inc., Natick, MA, United States) using PsychToolbox [27].

The required force was individually adjusted. Therefore, in each session, participants squeezed the force grip sensors as hard as possible to calculate their maximum voluntary force (MVF) for each hand. For the task runs participants were instructed to use 7–13 % of their MVF. Each task run consisted of 16 alternating fast and slow task blocks, with the starting order counterbalanced across the group (Fig. 1B). Blocks began with a 2 s instruction indicating the speed (fast/slow), followed by a 30 s task period during which participants performed coordinated movements in sync with the metronome sounds while fixating on a central cross. Participants then received 1s feedback on the force used (green for correct (7–13 % MVF), pink for excessive force (>13 % MVF) and blue for insufficient force (<7 % MVF); Fig. 1C). The rest blocks, where a fixation cross was shown for 15 s, preceded each task block and served as an implicit baseline in the fMRI block design.

Task performance was quantified using Pearson's correlation between the force-time course of both hands (see Supplementary Fig. S3 for an exemplary time course of one task block). During the first visit and during task training of the second visit, experimenters gave feedback until this correlation was sufficient (defined as $r < -0.53$ in the slow and $r < -0.37$ in the fast conditions; these threshold values were determined as 20 % above the mean values observed in a behavioural pilot study, see Supplementary Information; Pearson's r of −1 would represent perfectly alternating movements of the left and right hands). Feedback was also given to ensure that the speed of movement was 1.4–2.4 Hz in slow blocks (target 1.9 Hz) and 2.5–3.5 Hz in the fast blocks (target 3 Hz).

Linear mixed-effects models with speed and stimulation conditions as fixed-effect factors and volunteers as random-effect factors were performed in R (R Core Team, Vienna, Austria) using the lme4 package [28], with the mean Pearson correlation for each task speed and stimulation condition for each participant as the dependent variable. Any additional covariates were individually added as fixed effect factors to the model.

2.4. Transcranial alternating current stimulation

tACS was applied with a Starstim 8 (Neuroelectics, Barcelona, Spain). Visit 1 employed a simpler two-electrode montage at F4 and PO4. Two 40 mm diameter rubber electrodes were positioned using Ten20 paste. Visit 2 employed an 8-electrode montage, with 40 mm diameter rubber electrodes at C3/4, F3/4 and T7/8 and 23 mm diameter rubber electrodes at P3/4 (see Fig. 2A). The current at the central electrodes (i.e. C3/4) was phase-shifted 180° from the corresponding outer electrodes in both 3-in-1 montages, allowing us to target the M1s with low current leakage across hemispheres. Impedance at each electrode was kept below 10 kΩ.

In visit 1, the tACS current was increased in a stepwise fashion, to ensure that participants could tolerate 4 mA peak-to-peak comfortably. In visit 2, we performed a short (60 s) familiarisation tACS stimulation outside the MR scanner. During the MR-task runs, tACS was applied at 4 mA peak-to-peak at the C3/4 electrodes, with a 3 s ramp-up and ramp-down.

Three stimulation conditions were tested: zero-phase (ZP), jittered-phase (JP) and sham (SH) tACS. The order of stimulation conditions was counterbalanced across the group, and participants were blinded to

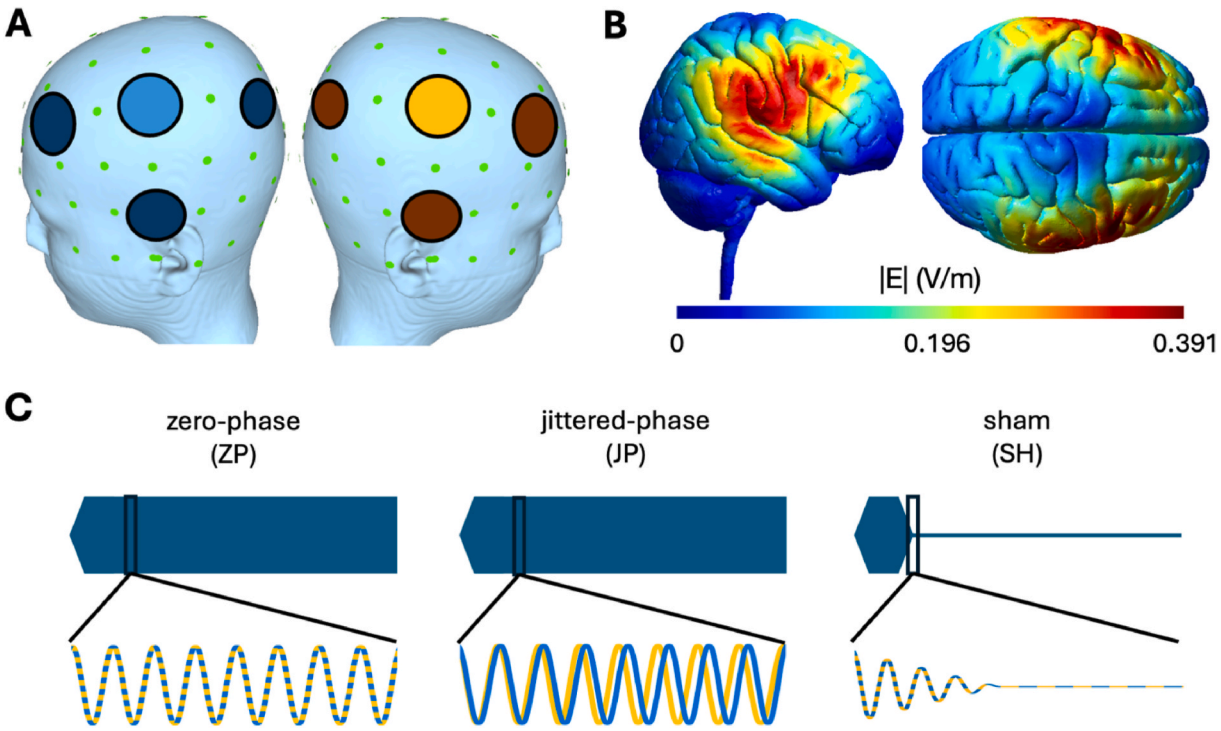

Fig. 2. Transcranial alternating current stimulation (tACS) setup. (A) tACS montage shown for the left and right hemisphere during the tACS-fMRI setup. Colours represent the phase shift: the inner electrodes over C4 (light orange) and over C3 (light blue) are shifted by 180° as compared to the respective outer electrodes, depicted in darker colours. This montage led to an E-field distribution on the MNI template for zero-phase (ZP) stimulation at 4 mA peak-to-peak as shown in (B). (C) Schematic overview of the tACS conditions: The waveforms of inner electrodes of the tACS, i.e. C3 as shown in blue and C4 as shown in orange, follow the same 20 Hz sinusoidal currents for the zero-phase (ZP) condition and two currents that independently changed their frequency between 19.5 and 20.5 Hz for the jittered-phase (JP) condition. The sham (SH) conditions consisted of a short (10 s) ZP stimulation followed by a 3 s ramp-down to zero. All conditions start with a 3 s ramp-in period.

the stimulation conditions. ZP stimulation used 20 Hz sinusoidal currents with phase offset zero (0° phase-lag) between the two hemispheres (see Fig. 2B for simulated E-field distributions). For JP stimulation two currents were applied that independently changed their frequency between 19.5 and 20.5 Hz, leading to continuous interhemispheric phase-shifts (Fig. 2C). These active stimulation conditions (ZP and JP) were applied over the whole course of the tACS-fMRI task run (approx. 13 min per condition). For SH stimulation, ZP stimulation was applied for 10 s followed by a 3 s ramp-down at the beginning of the tACS-fMRI task run. The length of ramp-up and -down as well as the length of the sham train differs across previous tACS studies (e.g. 30 s ramp-up and -down without a sham train [29–31], a 30 s sham train [32] or 10 s ramp-up and -down with a 3 s sham train [33]). We chose a 10 s sham train to ensure that participants felt sensations similar to the active tACS conditions and reached a usually observed habituation to these sensations.

2.4.1. *E-field simulations*

To quantify the E-field in M1 and to investigate whether interindividual differences influenced behaviour and fMRI readouts we conducted E-field simulations using SimNIBS 4.0.1 [34] on both the MNI template and individual anatomical scans. Individual head models were constructed from T1 and T2 scans using Charm [35]. tACS electrode artefacts were removed manually using ITK-SNAP (http://www.itksnap.org, [36]). The skin-air boundaries of the segmentations were then smoothed using a Gaussian smoothing kernel with a radius of 3 mm prior to running the simulations. For the simulations we defined the rubber electrodes with a thickness of 1 mm and a gel layer of 2 mm choosing the ellipse setting of [diameter, diameter] (diameter of 40 mm for bigger and 23 mm for smaller electrodes). Default settings were used for conductivities.

We extracted the maximum E-field strength and the absolute normal component across the entire grey matter (GM) sheet and within the M1s (region 4 from the HCP-MMP1 atlas [37]) from both the individual and MNI surface simulations. We also extracted the mean E-field within the GM in the seeds of left and right M1 as used for the psychophysiological interaction (PPI) analysis (see below), as well as in the precentral gyrus (as taken from the AAL atlas [38]).

2.5. *Magnetic resonance imaging*

2.5.1. *MR acquisition*

Whole-brain MR images were acquired on a Siemens Prisma 3T MRI system equipped with a 64-channel head coil. Task-related functional MR images were acquired using a multi-band echo planar imaging (MB-EPI, [39–41]) sequence (766 vol, TR = 1030 ms, TE = 37.4 ms, MB acceleration factor 6, flip angle = 60°, 72 coronal slices, FOV = 208x208x144 mm^3, voxel size = 2x2x2 mm^3). Additionally, one field map was acquired for every participant (TR = 607 ms, TE1 = 4.92 ms, TE2 = 7.38, flip angle = 46°, 62 coronal slices, FOV = 210x210x155 mm^3, voxel size = 2.5x2.5x2.5 mm^3). High-resolution T1-weighted 3D structural images (TR = 1900 ms, TE = 3.96 ms, flip angle: 8°, FOV = 232x256x192 mm^3, voxel size = 1x1x1 mm^3, 192 transversal slices) were acquired with a Magnetisation Prepared Rapid Acquisition Gradient Echo sequence and T2-weighted structural images (TR = 2500 ms, TE = 275 ms, flip angle: 8°, FOV = 272x272x191 mm^3, voxel size = 0.8x0.8x0.8 mm^3, 224 sagittal slices) without fat suppression.

2.5.2. *Task-related MR analyses: activation*

FMRI analyses were performed using FMRIB Software Library (FSL, Oxford; [42]). The following preprocessing steps were applied: B0 field map unwarping, motion-correction with MCFLIRT [43], slice-time correction, brain extraction using BET, grand-mean intensity

normalisation of the entire 4D dataset by a single multiplicative factor, and high-pass temporal filtering with a 100 s cut-off. The mean relative displacement was 0.10 ± 0.025 mm. The T1 images were bias-field corrected using fsl_anat. FMRI images were linearly registered to the individual T1 scan, via a task-run specific reference volume, and then non-linearly to the MNI152 template using FNIRT [42]. FIX (FMRIB's ICA-based Xnoiseifier [44,45], using the UK Biobank data training set, threshold of 20) was applied to denoise the data. Following denoising, the fMRI data was smoothed with a 5 mm FWHM Gaussian kernel and then modelled with a general linear model (GLM) with 5 explanatory variables (EVs): (EV 1) slow task blocks, (EV 2) fast task blocks, (EV 3) instruction screen, (EV 4) feedback screen and (EV 5) any instances of force values above 5 % of the individual maximum force during rest blocks. These EVs were convolved with the double-gamma haemodynamic response function, temporal derivatives were added, and temporal filtering was applied. Standard and extended motion parameters were added as confounds. The different sessions per participant were combined in a second-level FEAT analysis. Detailed descriptions of the contrasts are provided in the Supplementary Information.

We first identified a mean task activation network, independent of tACS and speed condition, using Mixed Effects (FLAME 1 + 2 [46]) with cluster-forming thresholds of Z = 2.3 and P = 0.01 on the group level. To define the M1 seeds for subsequent FC analyses, we then applied a pre-threshold mask of the bilateral A4ul regions (upper limb motor regions in the precentral gyrus) from the Brainnetome atlas (https://atlas.brainnetome.org, [47]) with cluster-forming thresholds of Z = 2.3 and P = 0.01.

Next, we compared the speed conditions (slow-fast) independent of tACS, using Mixed Effects (FLAME 1 + 2 [46]) with cluster-forming thresholds of Z = 2.3 and P = 0.01 on the group level. Then, to see whether stimulation effects on task-related activation have to be taken into account for the FC analyses, we ran a second-level analysis for each participant separately with fixed effects, contrasting the different tACS and speed conditions. At the group-level, we then conducted a Mixed Effects analysis using FLAME 1 + 2 [46]. To investigate the effects of tACS specifically on the motor-related cortex, we used a pre-threshold mask including motor cortical areas (bilateral pre- and postcentral areas, bilateral supplementary motor areas as defined in the AAL atlas [38]), with cluster-forming thresholds of Z = 2.3 and P = 0.01.

2.5.3. Task-related MR analyses: functional connectivity

Psychophysiological interaction (PPI) analyses were performed on the denoised and smoothed data to examine tACS-related changes in FC of task-specific peaks in bilateral M1s. To do this, we defined the left and right M1 seeds 8 mm radius spheres around the peak coordinates from the activation analysis detailed above.

Time courses were extracted from denoised data for M1 seeds and control regions in the cerebrospinal fluid (CSF) and white matter (WM). The first-level GLM for the FC analyses across speed conditions (slow + fast) included nine EVs: (EV 1) the psychological factor (slow and fast task blocks), (EV 2) the physiological factor (seed time course), (EV 3) the interaction term of the psychological and physiological factor (PPI), (EV 4) the instruction screen, (EV 5) the feedback screen and (EV 6) the force used during rest blocks (see above), the time course of the (EV 7) left CSF and the (EV 8) right CSF and of the (EV 9) WM. For the FC analyses comparing speed conditions (slow-fast) the psychological factor (EV 1) consisted of the slow task blocks modelled with +1 and the fast task blocks modelled with −1 and an additional EV (EV 10) was added for all task blocks (slow + fast). The EVs for the psychological factor, instruction screen, feedback screen, rest block force and those including task blocks were convolved with the double-gamma haemodynamic response function, temporal derivatives were added and temporal filtering applied. Additionally, standard and extended motion parameters were added as confounds. Second-level and group-level analyses were conducted as detailed above for the activation analyses.

Effect sizes were calculated per significant cluster by calculating paired Cohen's d from the extracted beta values for the corresponding pair of conditions.

2.5.4. Task-related MR analyses: regression analyses

Group-level analyses incorporated covariates, including sensation rating differences between conditions as covariate of no interest as a follow-up on the tACS effect on interhemispheric FC (see Results section). Additionally, we added mean E-field values within PPI seed regions during ZP as a covariate of interest in a more restrictive mask, including only the contralateral precentral and postcentral gyrus (AAL atlas). As JP stimulation has comparable E-field strengths to ZP stimulation [24], we assumed the same values for JP. Furthermore, even though no E-fields were applied during SH, we formally assigned the same E-field strengths for SH as simulated for ZP. We expected that we would not find any relationship between the E-field magnitude and the FC for the SH condition. Non-normally distributed covariates underwent Box-Cox transformation. All covariates were demeaned before inclusion in fMRI analyses. We applied cluster-forming thresholds of Z = 2.3 and P = 0.01.

3. Results

3.1. E-field simulations quantified M1 targeting

We first wanted to know whether our tACS montage was able to target the M1s bilaterally. Individual surface simulations revealed maximum field strengths of 0.45 ± 0.047 V/m across the grey matter, and 0.432 ± 0.050 V/m in M1s (99.9th percentile). The mean E-field values in the PPI M1 seeds were 0.095 ± 0.016 V/m and 0.089 ± 0.017 V/m for left and right seeds respectively.

3.2. 20 Hz tACS to bilateral M1 did not modulate behaviour significantly

Next, we investigated whether bi-hemispheric 20 Hz tACS modulated behaviour on our bimanual coordination task. A linear mixed-effects analysis of bimanual coordination, with one factor of speed (fast, slow) and one factor of stimulation (ZP, JP, SH) revealed a significant main effect of speed ($X^2(1) = 20.594$, $p < 0.001$, Cohen's $f^2 = 0.2080211$), such that participants performed better during the slow blocks compared to the fast ones ($t(86.1) = -4.746$, $p < 0.0001$, Cohen's $d = -0.9668785$, Fig. 3A), as would be expected. However, there was no main effect of stimulation ($X^2(2) = 1.0232$, $p = 0.60$, Cohen's $f^2 = 0.01044093$) and no speed by stimulation interaction ($X^2(2) = 1.8575$, $p = 0.40$, Cohen's $f^2 = 0.01895431$).

To determine whether the amplitude of the applied E-field was associated with behavioural effects, we added a covariate of interest as a fixed effect to our models. There was no main effect of the E-field in the precentral gyrus ($X^2(1) = 3.1165$, $p = 0.08$, Cohen's $f^2 = 0.03147967$), of the E-field in the PPI seeds (i.e., adding the E-fields of the left and right PPI seeds) ($X^2(1) = 0.204$, $p = 0.65$, Cohen's $f^2 = 0.002060711$), nor of the sensation ratings ($X^2(1) = 0.0381$, $p = 0.85$, Cohen's $f^2 = 0.0003852521$) on the coordination of the two hands.

To investigate whether tACS led to differences in force used in the task, we performed a linear mixed-effects analyses which revealed no speed by stimulation interaction ($X^2(2) = 0.3575$, $p = 0.84$, Cohen's $f^2 = 0.003647923$), no main effect of stimulation ($X^2(2) = 0.0448$, $p = 0.98$, Cohen's $f^2 = 0.0004573651$) and no main effect of speed ($X^2(1) = 1.2671$, $p = 0.26$, Cohen's $f^2 = 0.01279914$; see Fig. 3B).

3.3. tACS did not modulate task-related fMRI activation significantly

Before analysing task-related FC, we then wanted to determine whether bi-hemispheric 20 Hz tACS modulated task-related neural activation. We first determined which brain regions were active during task performance, independent of tACS condition or task level (see Supplementary Table S1 and Supplementary Fig. S4). As would be

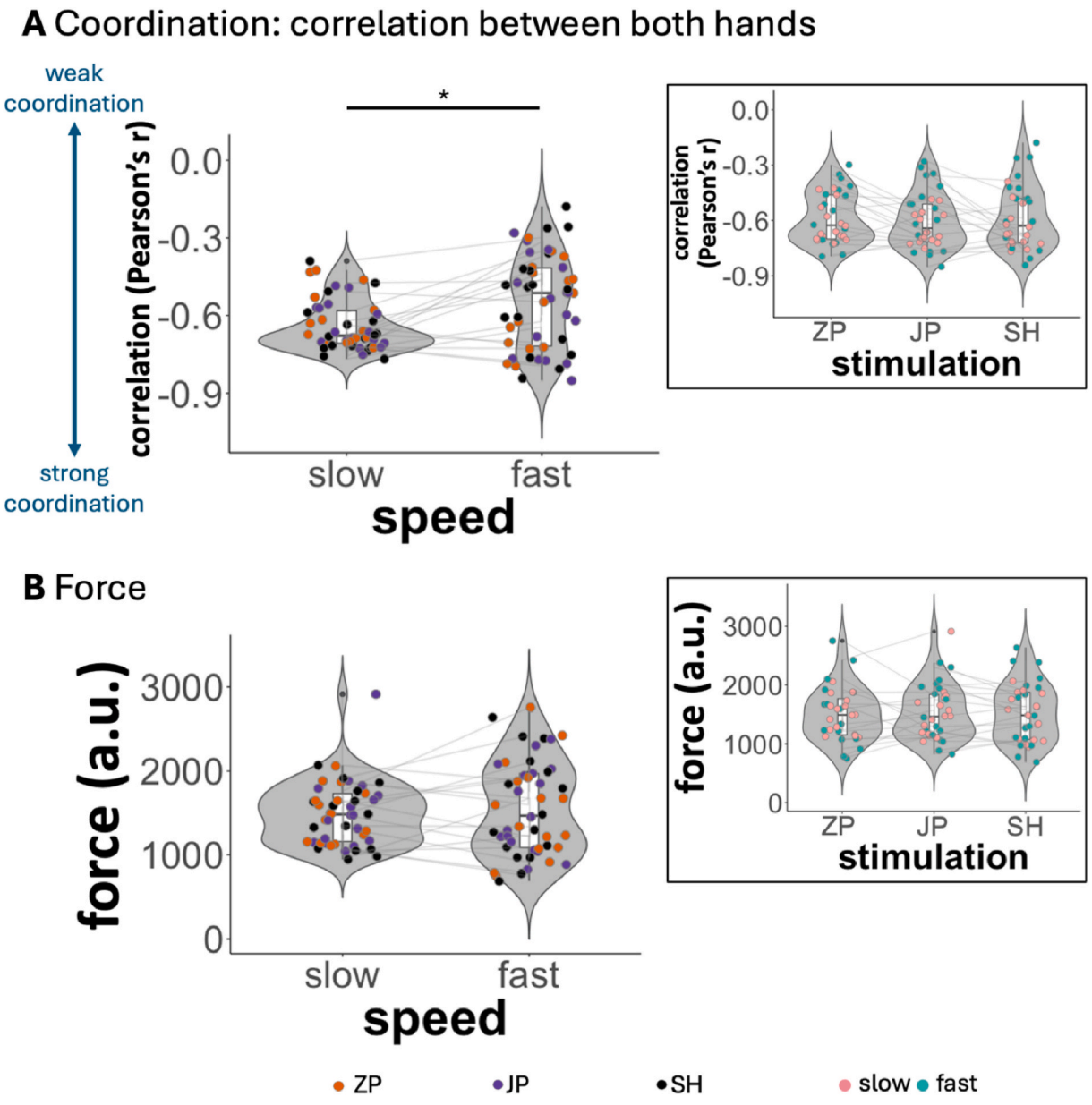

Fig. 3. Statistical model results for coordination and force. (A) For coordination, we observed a significant speed effect, showing better coordination (i.e., a correlation value (Pearson's r) of −1 would represent perfectly alternating movements of the left and right hands) during the slower as compared to the faster task blocks, but no stimulation-related effects. (B) The force levels were neither influenced by speed or stimulation. Filled circles (jittered horizontally within the respective violin plot) represent individual data and lines connect these across conditions for each participant. The shape of the violin plots and the included boxplots depict the distribution of the data. Asterisks (*) indicate significant statistical tests ($p < 0.05$). a.u. – arbitrary unit, tACS – transcranial alternating current stimulation, ZP – zero-phase tACS, JP – jittered-phase tACS, SH – sham tACS.

expected in this type of task, we saw task-related activations in multiple cortical and subcortical motor areas, including the primary motor cortex, premotor cortex, supplementary motor area (SMA), striatum and cerebellum. Next, we determined the brain regions that differed between task levels, independent of tACS conditions (see Supplementary Table S1 and Supplementary Fig. S5). We observed higher activation levels in the slow condition compared to the fast one, in multiple cortical and subcortical areas, including bilateral precentral and postcentral regions, superior parietal regions, SMA, caudate, thalamus, putamen, central opercular cortex, pallidum, insula and cerebellum. We observed higher activation in fast compared to slow conditions in several areas, including the frontal regions, (para)cingulate regions, occipital cortex, precuneus, inferior temporal areas, (para-)hippocampus, amygdala, insula and left cerebellum.

Critically, there were no significant differences in neural activation patterns in response to the motor task among the three stimulation conditions. Therefore, no stimulation effects on functional activation have to be taken into account for the subsequent FC analyses.

3.4. General task-related fMRI functional connectivity of the M1 seeds

To address our hypothesis that 20 Hz tACS to bilateral M1s modulates interhemispheric FC, we performed a PPI analysis. As detailed in the Methods section, we created 8 mm radius spherical seed regions in the left and right M1s, centred on as the mean centre of gravity of the task-related activity in each M1 separately (see Supplementary Table S2 and Fig. 4A).

First, we investigated the FC of the two motor cortices, independent

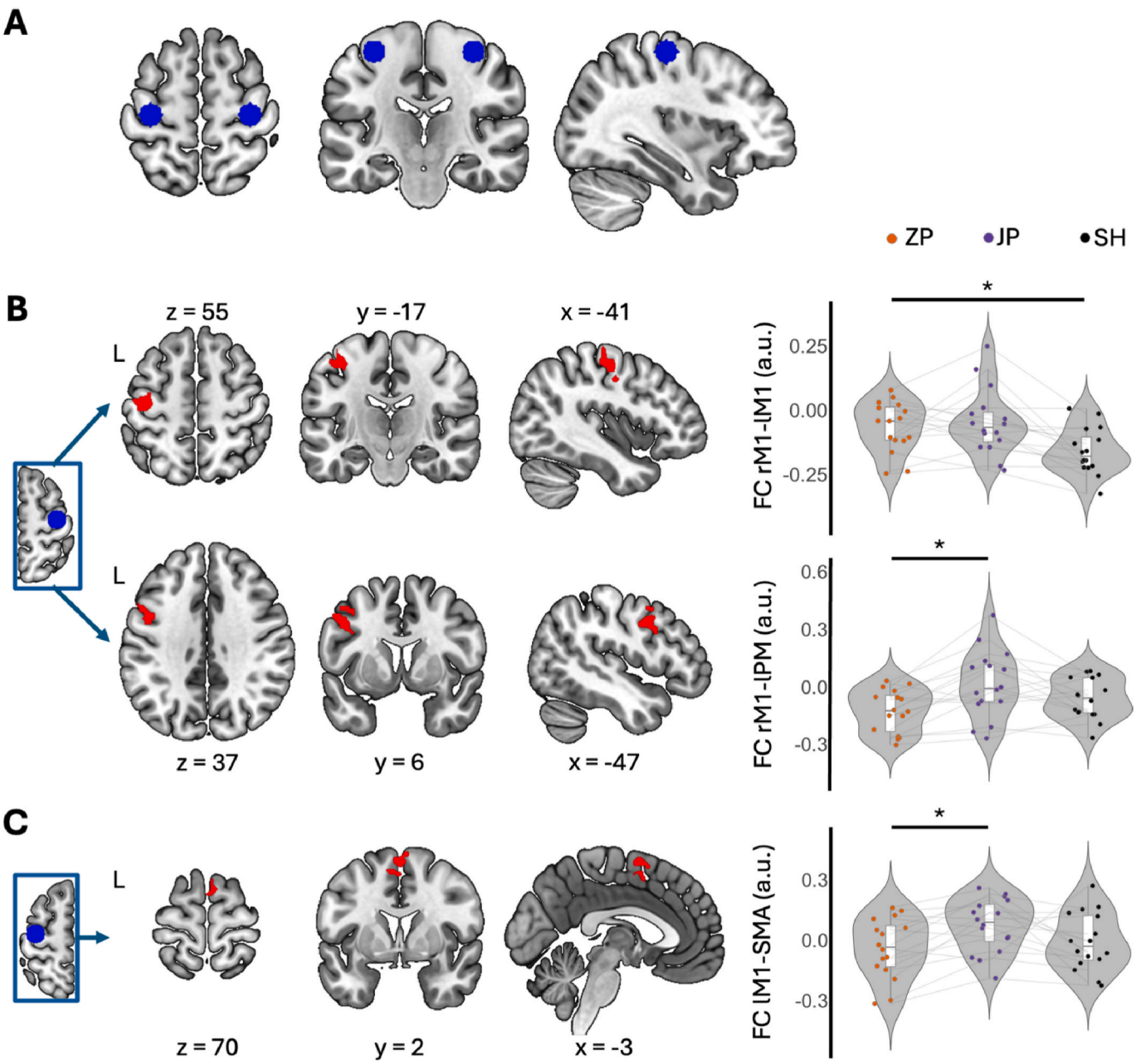

Fig. 4. Effects of tACS on functional connectivity. (A) Primary motor cortex (M1) seeds for the fMRI functional connectivity (FC) analyses: The 8 mm radius spheres used for the FC analyses are depicted in blue. (B) FC seeded in the right M1 (rM1) differed significantly in a left M1 (lM1) cluster between zero-phase (ZP) and sham (SH) conditions. The FC in SH was lower, i.e. negative, than in ZP. Additionally, the FC seeded in the right M1 differed significantly in a left premotor (lPM) cluster between zero-phase (ZP) and jittered-phase (JP) conditions, with higher FC in JP. (C) FC seeded in the left M1 differed significantly in a cluster in the supplementary motor area (SMA) between ZP and JP conditions, with higher FC in JP. The spheres and clusters are displayed on a T1-weighted template image (neurological convention). Filled circles (jittered horizontally within the respective violin plot) represent individual data and lines connect these across conditions for each participant. The shape of the violin plots and the boxplots depict the distribution of the data. Asterisks (*) indicate the contrast from which the fMRI clusters resulted. fMRI – functional magnetic resonance imaging.

of tACS condition or speed. Directly correlating the PPI time-courses revealed a significant negative FC between left and right M1 (see Supplementary Table S3.1 and S3.3 as well as Supplementary Fig. S6A and B). This negative FC pattern was stronger (i.e., had a larger absolute value) in the slow compared to the fast blocks (see Table S3.2 and S3.4 as well as Supplementary Fig. S6C and D). Additionally, both M1s were significantly negatively correlated with extensive regions stretching through the M1s and postcentral gyri bilaterally, and significantly positively correlated with clusters within ipsilateral M1. For the right M1 seed, the latter, positively correlated, ipsilateral M1 cluster extended into the SMA. Additionally, the FC between left M1 and SMA was higher in the fast compared to the slow blocks (see Supplementary Table S3 and Supplementary Fig. S6).

3.5. tACS modulated task-related functional connectivity between M1s

We next investigated what effect bilateral 20 Hz tACS would have on M1 FC patterns. Comparing FC patterns across speed conditions (i.e. combining slow and fast blocks) between different tACS conditions demonstrated that FC between the right and left M1 seeds was significantly different in the sham and ZP conditions, such that there was significantly less negative FC between left and right M1s in ZP compared

Table 1
Functional connectivity comparing tACS and speed conditions. Clusters were determined with cluster-forming thresholds of Z = 2.3 and P = 0.01 within the cortical motor regions (precentral and postcentral gyrus, premotor cortices (PM), supplementary motor area (SMA)). MNI – Montreal Neurological Institute.

Area	Cluster size (voxel)	Maximum *Z*-score	MNI coordinates (mm) of maximum *Z*-statistic		
			x	y	z
1. **PPI seeded in the right M1: slow + fast**					
ZP-SH (higher connectivity between right M1 and the following clusters in zero-phase as compared to sham tACS)					
Left M1	219	4.06	−44	−18	54
JP-ZP (higher connectivity between right M1 and the following clusters in jittered-phase as compared to zero-phase tACS)					
Left PM	334	3.48	−38	8	48
2. **PPI seeded in the right M1: slow-fast**					
No significant clusters					
3. **PPI seeded in the left M1: slow + fast**					
JP-ZP (higher connectivity between left M1 and the following clusters in jittered-phase as compared to zero-phase tACS)					
SMA	205	3.56	8	−10	76
4. **PPI seeded in the left M1: slow-fast**					
No significant clusters					

Table 2
Functional connectivity comparing tACS and speed conditions with sensations used as covariate of no interest: i.e., the corresponding difference between the sensation ratings of the pair of conditions used in the fMRI contrast. Clusters were determined with cluster-forming thresholds of Z = 2.3 and P = 0.01 within the cortical motor regions (precentral and postcentral gyrus, premotor cortices (PM), supplementary motor area (SMA)). MNI – Montreal Neurological Institute.

Area	Cluster size (voxel)	Maximum *Z*-score	MNI coordinates (mm) of maximum *Z*-statistic		
			x	y	z
1. **PPI seeded in the right M1: slow + fast covariate: difference in sensation ratings**					
ZP-SH, covariate of no interest: sensations ZP-SH					
Left M1	199	3.98	−44	−18	54
JP-ZP, covariate of no interest: sensations JP-ZP					
Left PM	311	3.43	−38	8	48
2. **PPI seeded in the left M1: slow + fast covariate: difference in sensation ratings**					
JP-ZP, covariate of no interest: sensations JP-ZP					
SMA	305	3.73	6	−10	74
Left postcentral gyrus	218	3.98	38	−38	62

with sham tACS (see Fig. 4B upper part and Table 1.1; Cohen's d = 1.03). There was no significant difference between JP and ZP conditions, nor between JP and SH conditions at the chosen thresholds.

We observed a difference between sham and active stimulation conditions in terms of the sensations evoked (see Supplementary Information). To ensure that the differences in FC described above could not be simply explained by differences in sensation, we ran a control analysis including sensation rating as a covariate of no interest. The significant cluster described above remained significant after controlling for sensation ratings (see Table 2.1 in comparison to Table 1.1).

Next, we wanted to know whether the effects of tACS on task-related FC were dependent on the level of engagement of the network in the task being performed. We therefore used the speed condition difference (slow-fast) as the psychological factor of the PPI analyses described previously. For either the right or left M1 seed PPIs, we observed no significant clusters when comparing the different tACS conditions between speed conditions (slow-fast).

3.6. tACS modulated task-related functional connectivity between M1s and the rest of the motor network

We then wanted to investigate whether bilateral M1 tACS led to a change in how the M1 connected with the rest of the motor network. Key to our hypothesis was that there would be a different effect of ZP and JP on FC. Indeed, ZP and JP differentially modulated FC between right M1 and left premotor cortex (PM), such that the FC was stronger during JP than during ZP (see Table 1.1 and Fig. 4B lower part; Cohen's d = 1.09). The same analysis seeded in the left M1 revealed a difference in FC between left M1 and the supplementary motor area (SMA) when comparing JP and ZP conditions (see Table 1.3 and Fig. 4C; Cohen's d = 1.01). Here, again, FC between left M1 and SMA was stronger during JP than during ZP. The tACS effects in FC did not differ between the speed conditions for either the right or left M1 seeds.

The significant clusters described above remained significant after controlling for sensation differences evoked by tACS (see Table 2 in comparison to Table 1). In addition, we observed an additional cluster in the left post-central gyrus where intrahemispheric FC with the left M1 PPI seed significantly differed between ZP and JP tACS (see Table 2.2).

3.7. Relationship between functional connectivity and individual E-field strengths

Finally, we tested whether there was a direct relation between E-field strength and interhemispheric FC changes due to tACS. We therefore added the individual simulated E-field strength for ZP within the GM of the seed region as a covariate of interest to the PPI analyses. When considering the task demand, i.e. comparing the slow and fast conditions (PPI slow-fast), we observed a significant difference between ZP and SH conditions in the correlation between the applied ZP E-field magnitude in the right M1 and right M1 FC with the contralateral left M1 (see Table 3.2 and Fig. 5A). Interestingly, this effect was driven by the significant relationship between ZP E-field in the right M1 seed and the FC of the right M1 seed with the left M1 cluster in the ZP slow condition (SH slow: t(14) = 1.116, $p_{uncorrected}$ = 0.2832; SH fast: t(14) = -0.93509, $p_{uncorrected}$ = 0.3656; ZP slow: t(14) = -3.1706, $p_{uncorrected}$ = 0.006807; ZP fast: t(14) = 0.92527, $p_{uncorrected}$ = 0.3705; see Fig. 5B). Specifically, higher ZP E-field values related to stronger negative FC during the ZP slow condition.

4. Discussion

In this study, we combined a high-definition dual-site transcranial alternating current (tACS) setup at 4 mA with a concurrent functional magnetic resonance imaging (fMRI) design, to investigate changes in functional connectivity (FC) during tACS. We targeted the bilateral primary motor cortices (M1s) during a bimanual motor coordination

Table 3
Functional connectivity comparing tACS and speed conditions with ZP E-field in the PPI seed used as covariate. Clusters were determined with cluster-forming thresholds of Z = 2.3 and P = 0.01 within the contralateral primary sensorimotor regions (precentral and postcentral gyrus). MNI – Montreal Neurological Institute.

Area	Cluster size (voxel)	Maximum *Z*-score	MNI coordinates (mm) of maximum *Z*-statistic		
			x	y	z
1. **PPI seeded in the right M1: slow + fast**					
Covariate of interest: ZP E- field strength in the right M1 seed					
No significant clusters					
2. **PPI seeded in the right M1: slow-fast**					
Covariate of interest: ZP E- field strength in the right M1 seed					
SH-ZP					
Left M1	250	3.9	−62	−18	34
3. **PPI seeded in the left M1: slow + fast**					
Covariate of interest: ZP E- field strength in the left M1 seed					
No significant clusters					
4. **PPI seeded in the left M1: slow-fast**					
Covariate of interest: ZP E- field strength in the left M1 seed					
No significant clusters					

task, thus enabling the investigation of active motor networks. Contrary to our expectation, we did not observe any significant tACS effects on behaviour. However, we found an attenuation effect of zero-phase (ZP) tACS on interhemispheric FC. Additionally, the task-related M1 FC with other motor cortical regions (premotor cortex (PM) and supplementary motor area (SMA)) differed between the two active types of stimulation. Finally, individual E-field strengths correlated with interhemispheric FC in the ZP condition, depending on task demand.

4.1. Attenuated interhemispheric connectivity

Our results suggest that ZP tACS attenuated interhemispheric FC between M1s compared to sham stimulation. This deviates from our hypotheses expecting a strengthening in interhemispheric FC between the M1s during ZP tACS and an attenuation in FC during jittered-phase (JP) tACS. As the underlying FC between both M1s was negative during the execution of this specific asymmetrical coordination task, the application of ZP tACS might have attenuated negative FC towards

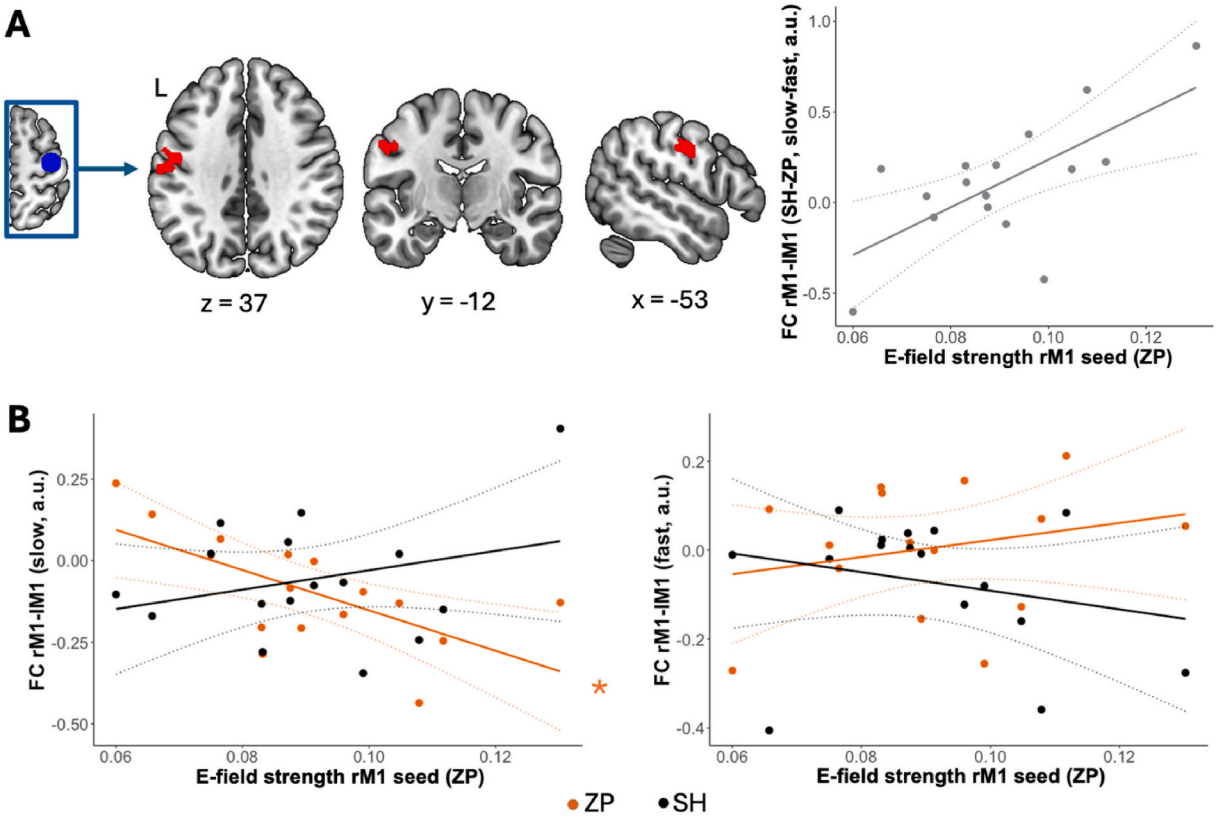

Fig. 5. *Modulation of relationship between ZP E-field strength in right M1seed and functional connectivity by tACS.* (A) The relationship between the applied ZP E-field magnitude in the right M1 (rM1) and right M1 functional connectivity (FC) with the contralateral left M1 (lM1) differed significantly between ZP and SH conditions when comparing the slow and fast conditions. The clusters are displayed on a T1-weighted template image (neurological convention). (B) Follow-up tests showed a significant relationship between ZP E-field strength and FC only in the ZP slow condition. Asterisks (*) indicate significant relationships (Pearson's correlation with $p < 0.05$) between the FC and covariate values in individual conditions (e.g. ZP slow). Note that the raw E-field strength values are depicted on the plots rather than the demeaned values used as covariates for the analyses. Filled circles represent individual data, solid lines depict the linear regression fits, and dotted lines represent the 95 % prediction intervals of the linear function. M1 – primary motor cortex, tACS – transcranial alternating current stimulation, ZP – zero-phase tACS, SH – sham tACS, a.u. – arbitrary unit.

positive FC by applying the identical stimulation above both regions. Similarly, unifocal beta tACS disrupted the normally observed relationship between interhemispheric M1 FC and the rest of the motor network [12]. A recent study reported increased interhemispheric inhibition (IHI) between the M1s (as measured with transcranial magnetic stimulation) after ZP 20 Hz tACS [30]. While it is difficult to directly translate this result to fMRI FC, this might point to a more complex effect of ZP tACS on interhemispheric FC, which is worth exploring with multimodal approaches. Specifically, IHI has been shown at a shorter (10 ms) and longer (40 ms) time lag between both M1s [48] but the directionality of this effect in the current task is, to the best of our knowledge, not known. Additionally, as a relationship between IHI and GABA-ergic circuits has been suggested [49] the addition of MR spectroscopy would be a suitable extension for future research. Furthermore, future studies should also investigate the effects of further phase lags, such as taking into account the known short and long IHI values of 10 ms and 40 ms, as well as pi-phase tACS, which might be, speculatively, more closely related to negative FC as measured with fMRI. In the future, personalized computational models or individual IHI measurements could help to estimate the optimal phase lag for each participant.

Alternatively, the attenuation effect of ZP tACS might be explained by our use of a fixed tACS frequency (20 Hz) for all the participants. Instead of entraining the underlying oscillations to the applied 20 Hz rhythm, we might have introduced a strong and consistent noise factor attenuating the underlying negative FC between both M1s. Thus, individualized ZP tACS might enhance ongoing FC and associated behaviour. Similarly, previous studies showed that individualized-frequency alpha tACS over both M1s increased resting-state connectivity [8], while fixed-frequency unifocal beta tACS disrupted the relationship between interhemispheric M1 FC and the rest of the motor network [12]. In addition, a recent study has shown that the interplay of interregional conduction delays and stimulation frequency is critical for the effects of dual-site tACS on stimulation-outlasting EEG FC changes [50]. Heterogeneity in the individual conduction delays between the M1s could thus further contribute to variability in our data.

Conversely, JP tACS did not significantly attenuate interhemispheric FC at the chosen thresholds, as compared to sham or ZP tACS. While JP tACS might also introduce noise and result in numerically less strong negative interhemispheric FC (as seen in Fig. 4B), this response may not be consistent enough to lead to significant effects. In line with this, a recent study showed that ZP tACS resulted in stronger effects on FC than JP tACS in a resting-state tACS-EEG study [24].

4.2. Motor-network effects in response to tACS

Modifying brain dynamics may come along with compensatory and adaptive effects. Accordingly, we found further tACS-related responses that were revealed in the brain imaging analyses. Specifically, the FC between M1 seeds and PM as well as SMA differed between the two active tACS conditions. While these effects do not directly explain how the attenuated interhemispheric FC as compared to the sham condition was counteracted in the ZP condition, they might point to broader compensatory mechanisms involving different recruitment strategies within the motor cortical network under different types of dual-site tACS to maintain behavioural performance levels. However, all observed changes in FC might also represent an epiphenomenon and not be functional relevant, in light of the behavioural null finding.

The spread of tACS effects through the (cortical and subcortical) motor networks is in line with previous work in M1 tACS-fMRI studies using beta [8,12] as well as mu [51] tACS. Additionally, PM and SMA might be more strongly coupled to M1 in JP than in ZP condition due to the lower predictability of the JP stimulation. The SMA is thought to be involved in internally-guided movements, reflecting the coordination between both hands in our task, and indeed is a key node for bimanual coordination. The PM in externally-guided movements, reflecting the speed-adjustment towards the metronome sounds (e.g. [52–54]). The increased connectivity between M1 and these higher-order processing regions may therefore reflect a compensatory mechanism to maintain behaviour in the presence of a higher cognitive load required to counteract the unpredictable noise introduced by JP tACS.

Interestingly, tACS effects on FC did not differ between task demand levels, suggesting that initial differences in recruitment across fast and slow conditions did not lead to speed-specific tACS modulations. Importantly, even though the participants rated the sensations stronger for active than for sham conditions, the observed effects were not statistically driven by these sensations. Furthermore, given the overall sensation ratings and the absence of any adverse events, we conclude that our high-intensity tACS-fMRI setup was overall well tolerable. At the same time, we cannot fully exclude that subthreshold activation of sensory neurons during active tACS, es elicited by higher sensations on the head, might have modulated functional connectivity. Therefore, to avoid possible influences of different sensations in different tACS conditions, future studies could focus on better blinding mechanisms, such as applying a numbing cream underneath the tACS electrodes.

4.3. Relationship between interhemispheric connectivity and the E-field strength

The effects of tACS are known to be variable, at least in part due to the varying intensity of the electrical fields within the cortex. Therefore, we investigated whether the variation between participants in the E-fields applied to M1 may have influenced patterns of FC changes. We demonstrated speed-specific tACS modulation of the relationship between interhemispheric FC and ZP E-field strength. Specifically, there was only a significant relationship between ZP E-field strength and interhemispheric FC during ZP tACS in the slow condition. Our analyses demonstrated that the slow condition led to greater activity in the motor cortex and showed stronger negative FC, than the fast condition. These findings might seem counterintuitive but may result from more focus on “proper” motor control in the slow condition and from less control, decreased coordination and a greater cognitive load in the fast condition.

The strong and consistent interhemispheric bilateral M1 recruitment during slow coordination might then be more susceptible to attenuation than that seen in the fast condition, as there is more room for such modulations. Specifically, lower E-fields in the ZP condition showed stronger attenuation of the negative FC in the lateral left M1. This finding suggests that, in this specific region, we do not see an attenuation effect of ZP tACS overall, but possibly an attenuation effect emerges only at lower E-fields. This hypothesis might be supported by recent theories on the working mechanism of tACS, suggesting that tACS at lower E-fields desynchronises the underlying neural responses rather than synchronising responses to the applied current, as would be expected for higher E-fields [18]. Such desynchronisation might promote attenuation effects of the underlying FC. While JP tACS produced similar E-fields as ZP tACS, the JP stimulation pattern might not show similar effects on the (de)synchronisation of underlying neural responses.

4.4. Asymmetry in tACS effects

Notably, while the bimanual coordination task execution as well as the stimulation were symmetrical, the results reveal an asymmetry in tACS effects. Specifically, tACS-related FC patterns differed between left and right M1 seeds. This may be explained by the right-handedness of our participants. Additionally, motor skills do not recruit motor regions symmetrically due to hemispheric dominance [55]. Similarly, a current M1 tACS-fMRI study also showed asymmetrical results for mu tACS effects on task-related FC seeded in the targeted left and right M1 [51].

4.5. Active tACS did not modulate motor performance or activation significantly

Neither ZP nor JP tACS modulated motor performance during the bimanual coordination task. These results suggest that dual-site tACS over both M1s does not necessarily lead to changes in motor performance. One theoretically possible explanation is that bimanual coordination is not causally linked to FC of the M1s. A second option is that the observed modulations in FC were not strong enough to alter behaviour in the investigated task setup. Consequently, the observed changes in functional connectivity might be an epiphenomenon in the light of a null result in behaviour. Furthermore, another explanation, especially considering the attenuated interhemispheric FC in the ZP condition and further tACS effects on FC when comparing the active tACS conditions, is the use of compensatory mechanisms and differential recruitment of these other brain regions. However, while the tACS current is stronger here than in most other studies, the frequency was not individualized. Even though we used high-definition montages, E-fields were not only focused in the M1s, and showed inter-participant variability. All these considerations might explain a high variability in effects leading to a null result on the behavioural level. Similarly, the effects of bilateral M1 beta tACS showed inconsistent results in the literature: while some researchers observed behavioural effects on motor tasks using bilateral beta [30,56] M1 tACS, others could not [33,57,58]. At this point the literature on bilateral M1 tACS in the beta band during motor tasks is stills scarce, especially for high-definition montages. More research is needed to pinpoint the exact working mechanisms to reveal dual-site M1 beta tACS effects on motor tasks and whether these differ across different types of tasks (such as bimanual motor control, visuomotor tasks or motor learning) and phase-lags between the hemispheres. Additionally, other frequency bands, such as alpha and mu have shown promise to modulate motor behaviour with bilateral M1 tACS [51,56].

Similarly, while we observed tACS effects on FC, we did not see any significant tACS-related effects on fMRI activation, representing a null result on the activation level. Presumably tACS, and specifically dual-site tACS, alters FC more than activation as observed with fMRI. This is in accordance with previous literature on tACS-fMRI using unifocal beta tACS over M1 showing tACS modulations of FC in the absence of effects on activation [12]. While alpha tACS-fMRI studies showed changes in BOLD activation, these effects were subtle and might depend strongly on the specific target regions, phase-lags between dual-site tACS regions and appear to be state-dependent [59,60]. Furthermore, a recent study [61] indicated that tACS may have the most dominant effect on long-range projections rather than on local spiking. While this new finding is generally in line with our results of tACS modulating connectivity more than local activity, it could also imply that projections to other regions may have been stimulated additionally.

4.6. Considerations

Due to the setup of the current study, the sample size only allows us to investigate rather large effect sizes and limits the claims we are able to make as to whether our tACS approach might have small but significant effects on behaviour with a larger sample size. Future studies should try to collect a larger sample to look into more fine-grained effects of dual-site tACS on bimanual coordination. While we do not expect after-effects of phase-lag dependent modulations in functional connectivity resulting from the dual-site tACS intervention to outlast the time between tACS-fMRI task runs (of at least 5 min, including either a T1 or T2 measurement and instructions) based on previous research [24], we acknowledge that other studies indeed showed longer lasting tACS effects on EEG power [62–66]. However, the counterbalanced design attenuates influences of possible after-effects. Importantly, we did not observe any order effects in the described fMRI clusters (see Supplementary Information). In addition, we cannot exclude the possibility that the 10 s tACS in the sham condition may have influenced activity or functional connectivity, weakening the contrast of sham vs active stimulation.

Moreover, due to constraints of separating the left and right hemisphere E-field through the chosen tACS montage and using large rubber electrodes for comfort during the stimulation, the resulting E-field was rather widespread and not only focalised to M1 (see Supplementary Fig. S7 for the group average E-field map). Nevertheless, the E-field covered large parts of M1 and our study showed effects of task-related M1 functional connectivity. Furthermore, as common for fMRI analyses, we cannot exclude the possibility that the reported results may depend on the choices made for preprocessing and statistical parameters. Finally, future studies should integrate mechanistic measures, such as individual IHI measures (see above), to strengthen causal interpretations.

5. Conclusions

Our study showed that high-definition dual-site beta-tACS over both primary motor cortices altered functional connectivity between motor areas. However, this effect did not translate to the behavioural level. Altogether, dual-site tACS has the general potential for connectivity modulation, which is very important for neuroscientific studies as well as for clinical translations, not limited to the motor system. At the same time, more research is necessary to understand the complex mechanisms of dual-site tACS.

CRediT authorship contribution statement

Mareike A. Gann: Writing – review & editing, Writing – original draft, Visualization, Software, Resources, Methodology, Investigation, Formal analysis, Data curation, Conceptualization. **Ilenia Paparella:** Writing – review & editing, Methodology, Investigation. **Catharina Zich:** Writing – review & editing, Resources, Conceptualization. **Ioana-Florentina Grigoras:** Writing – review & editing, Software, Methodology, Formal analysis, Data curation. **Silvana Huertas-Penen:** Writing – review & editing, Software, Data curation. **Sebastian W. Rieger:** Writing – review & editing, Methodology, Conceptualization. **Axel Thielscher:** Writing – review & editing, Software. **Andrew Sharott:** Writing – review & editing, Funding acquisition, Conceptualization. **Charlotte J. Stagg:** Writing – review & editing, Writing – original draft, Validation, Supervision, Software, Resources, Project administration, Investigation, Funding acquisition, Formal analysis, Data curation, Conceptualization. **Bettina C. Schwab:** Writing – review & editing, Writing – original draft, Validation, Supervision, Software, Resources, Project administration, Investigation, Funding acquisition, Formal analysis, Data curation, Conceptualization.

Data Availability

At the time of publication, group fMRI statistical outputs mapped to standard space, as well as image and data processing pipelines from our study are freely available at the Data Sharing Platform of MRC Brain Network Dynamics Unit (https://data.mrc.ox.ac.uk/) under https://doi.org/10.60964/bndu-mw4b-t114 [67].

Declaration of competing interest

The authors declare that they have no known competing financial interests or personal relationships that could have appeared to influence the work reported in this paper.

Acknowledgements

This work was supported by the German Research Foundation (DFG, grant number SCHW 2023/2-1 to B.C.S.), the European Research Council (ERC StG DECODE, grant number 101116047, to B.C.S.), the Medical Sciences Internal Fund: Pump-Priming (grant number 0011905

to A.S.) of the University of Oxford, the Medical Research Council UK (MC_UU_00003/6 to A.S.), a Wellcome Trust Senior Research Fellowship (224430/Z/21/Z to C.J.S), the Sofina Boël Fund for Education and Talent (to I.P.), the F.R.S.-FNRS (to I.P.), the National Institute for Health Research (NIHR) Oxford Biomedical Research Centre and the NIHR Oxford Health Biomedical Research Centre (NIHR203316). A.T. was supported by the Lundbeck Foundation (grants R313-2019-622 and R244-2017-196) and the German Research Foundation (Research Unit 5429/1 (467143400), TH 1330/6-1 and TH 1330/7-1). The views expressed are those of the author(s) and not necessarily those of the NIHR or the Department of Health and Social Care. The Wellcome Centre for Integrative Neuroimaging is supported by core funding from the Wellcome Trust (203139/Z/16/Z and 203139/A/16/Z). For the purpose of Open Access, the author has applied a CC BY public copyright licence to any Author Accepted Manuscript (AAM) version arising from this submission. Additionally, we acknowledge the receipt of software for using multiband fMRI sequences from the University of Minnesota Center for Magnetic Resonance Research.

We thank all involved students and colleagues for assistance with data collection. We thank the WIN radiographers for imaging assistance. We thank Saad Jbabdi and Eik Vettorazzi for analysis assistance.

Appendix A. Supplementary data

Supplementary data to this article can be found online at https://doi.org/10.1016/j.brs.2025.08.011.

References

[1] Mišić B. Sporns Olaf From regions to connections and networks: new bridges between brain and behavior. Curr Opin Neurobiol 2016;40:1-7.
[2] Perich MG, Rajan K. Rethinking brain-wide interactions through multi-region 'network of networks' models. Curr Opin Neurobiol 2020 Dec;65:146–51.
[3] Serrien DJ, Brown P. The functional role of interhemispheric synchronization in the control of bimanual timing tasks. 2002.
[4] Grefkes C, Eickhoff SB, Nowak DA, Dafotakis M, Fink GR. Dynamic intra- and interhemispheric interactions during unilateral and bilateral hand movements assessed with fMRI and DCM. Neuroimage 2008 Jul;41(4):1382–94.
[5] Daffertshofer A, Peper C, Lieke E, Beek PJ. Stabilization of bimanual coordination due to active interhemispheric inhibition: a dynamical account. Biol Cybern 2005 Feb;92(2):101–9.
[6] Donchin O, Gribova A, Steinberg O, Bergman H, Vaadia E. Primary motor cortex is involved in bimanual coordination. Nature 1998 Sep;395(6699):274–8.
[7] Houweling S, Van Dijk BW, Beek PJ, Daffertshofer A. Cortico-spinal synchronization reflects changes in performance when learning a complex bimanual task. Neuroimage 2010 Feb;49(4):3269–75.
[8] Bächinger M, Zerbi V, Moisa M, Polania R, Liu Q, Mantini D, et al. Concurrent tACS-fMRI reveals causal influence of power synchronized neural activity on resting state fMRI connectivity. J Neurosci 2017 May 3;37(18):4766 LP–4777.
[9] Bergmann TO, Karabanov A, Hartwigsen G, Thielscher A, Siebner HR. Combining non-invasive transcranial brain stimulation with neuroimaging and electrophysiology: current approaches and future perspectives. Neuroimage 2016 Oct;140:4–19.
[10] Polanía R., Nitsche M.A., Ruff C.C. Studying and modifying brain function with non-invasive brain stimulation. Nat Neurosci [Internet] 2018;21:174-187. http://www.nature.com/articles/s41593-017-0054-4.
[11] To WT, De Ridder D, Hart Jr J, Vanneste S. Changing brain networks through non-invasive neuromodulation. Front Hum Neurosci 2018 Apr 13;12:128.
[12] Weinrich CA, Brittain JS, Nowak M, Salimi-Khorshidi R, Brown P, Stagg CJ. Modulation of long-range connectivity patterns via frequency-specific stimulation of human cortex. Curr Biol 2017;27(19):3061–3068.e3.
[13] Bradley C, Nydam AS, Dux PE, Mattingley JB. State-dependent effects of neural stimulation on brain function and cognition. Nat Rev Neurosci 2022 Aug;23(8):459–75.
[14] Fiene M, Schwab BC, Misselhorn J, Herrmann CS, Schneider TR, Engel AK. Phase-specific manipulation of rhythmic brain activity by transcranial alternating current stimulation. Brain Stimulat 2020;13(5):1254–62.
[15] Fiene M, Radecke JO, Misselhorn J, Sengelmann M, Herrmann CS, Schneider TR, et al. tACS phase-specifically biases brightness perception of flickering light. Brain Stimulat 2022 Jan;15(1):244–53.
[16] Antal A, Bikson M, Datta A, Lafon B, Dechent P, Parra LC, et al. Imaging artifacts induced by electrical stimulation during conventional fMRI of the brain. Neuroimage 2014 Jan;85:1040–7.
[17] Wischnewski M, Alekseichuk I, Opitz A. Neurocognitive, physiological, and biophysical effects of transcranial alternating current stimulation. Trends Cogn Sci 2022 Dec;S1364661322002984.
[18] Krause MR, Vieira PG, Thivierge JP, Pack CC. Brain stimulation competes with ongoing oscillations for control of spike timing in the primate brainLuo H, editor. PLoS Biol 2022 May 25;20(5):e3001650.
[19] Liu A, Vöröslakos M, Kronberg G, Henin S, Krause MR, Huang Y, et al. Immediate neurophysiological effects of transcranial electrical stimulation. Nat Commun 2018 Dec 1;9(1).
[20] Kang N., Ko D.K., Cauraugh J.H. Bimanual motor impairments in older adults: an updated systematic review and meta-analysis. EXCLI J 2022;21:1068-1083. ISSN 1611-2156 [Internet] https://www.excli.de/index.php/excli/article/view/5236. [Accessed 17 July 2024].
[21] Kim RK, Kang N. Bimanual coordination functions between paretic and nonparetic arms: a systematic review and meta-analysis. J Stroke Cerebrovasc Dis 2020 Feb;29(2):104544.
[22] Nettersheim FS, Loehrer PA, Weber I, Jung F, Dembek TA, Pelzer EA, et al. Dopamine substitution alters effective connectivity of cortical prefrontal, premotor, and motor regions during complex bimanual finger movements in Parkinson's disease. Neuroimage 2019 Apr;190:118–32.
[23] Patel P, Lodha N. Functional implications of impaired bimanual force coordination in chronic stroke. Neurosci Lett 2020 Nov;738:135387.
[24] Schwab BC, Misselhorn J, Engel AK. Modulation of large-scale cortical coupling by transcranial alternating current stimulation. Brain Stimulat 2019;12(5):1187–96.
[25] Reinhart RMG. Disruption and rescue of interareal theta phase coupling and adaptive behavior. Proc Natl Acad Sci 2017 Oct 24;114(43):11542–7.
[26] Reinhart RMG, Nguyen JA. Working memory revived in older adults by synchronizing rhythmic brain circuits. Nat Neurosci 2019 May;22(5):820–7.
[27] Brainard DH. The psychophysics toolbox. Spat Vis 1997;10(4):433–6.
[28] Bates D, Mächler M, Bolker B, Walker S. Fitting linear mixed-effects models using **lme4**. J Stat Softw [Internet] 2015;67(1). http://www.jstatsoft.org/v67/i01/. [Accessed 30 July 2024].
[29] Van Hoornweder S, Mora DAB, Nuyts M, Cuypers K, Verstraelen S, Meesen R. The causal role of beta band desynchronization: individualized high-definition transcranial alternating current stimulation improves bimanual motor control [internet]. http://biorxiv.org/lookup/doi/10.1101/2024.10.30.621096. [Accessed 7 January 2025].
[30] Lebihan B, Mobers L, Daley S, Battle R, Leclercq N, Misic K, et al. Bifocal tACS over the primary sensorimotor cortices increases interhemispheric inhibition and improves bimanual dexterity. Cerebr Cortex 2025 Feb 3:bhaf011.
[31] Cappon D, D'Ostilio K, Garraux G, Rothwell J, Bisiacchi P. Effects of 10 Hz and 20 Hz transcranial alternating current stimulation on automatic motor control. Brain Stimulat 2016 Jul;9(4):518–24.
[32] Pollok B, Boysen AC, Krause V. The effect of transcranial alternating current stimulation (tACS) at alpha and beta frequency on motor learning. Behav Brain Res 2015 Oct;293:234–40.
[33] Schoenfeld MJ, Grigoras IF, Stagg CJ, Zich C. Investigating different levels of bimanual interaction with a novel motor learning task: a behavioural and transcranial alternating current stimulation study. Front Hum Neurosci 2021;15(November):1–16.
[34] Thielscher A, Antunes A, Saturnino GB. Field modeling for transcranial magnetic stimulation: a useful tool to understand the physiological effects of TMS?. In: 2015 37th annual international conference of the IEEE engineering in medicine and biology society (EMBC) [internet]. Milan: IEEE; 2015. p. 222–5. http://ieeexplore.ieee.org/document/7318340/. [Accessed 30 July 2024].
[35] Puonti O, Van Leemput K, Saturnino GB, Siebner HR, Madsen KH, Thielscher A. Accurate and robust whole-head segmentation from magnetic resonance images for individualized head modeling. Neuroimage 2020 Oct;219:117044.
[36] Yushkevich PA, Piven J, Hazlett HC, Smith RG, Ho S, Gee JC, et al. User-guided 3D active contour segmentation of anatomical structures: significantly improved efficiency and reliability. Neuroimage 2006 Jul;31(3):1116–28.
[37] Glasser MF, Coalson TS, Robinson EC, Hacker CD, Harwell J, Yacoub E, et al. A multi-modal parcellation of human cerebral cortex. Nature 2016 Aug;536(7615):171–8.
[38] Tzourio-Mazoyer N, Landeau B, Papathanassiou D, Crivello F, Etard O, Delcroix N, et al. Automated anatomical labeling of activations in SPM using a macroscopic anatomical parcellation of the MNI MRI single-subject brain. Neuroimage 2002 Jan;15(1):273–89.
[39] Moeller S, Yacoub E, Olman CA, Auerbach E, Strupp J, Harel N, et al. Multiband multislice GE-EPI at 7 tesla, with 16-fold acceleration using partial parallel imaging with application to high spatial and temporal whole-brain fMRI. Magn Reson Med 2010 May;63(5):1144–53.
[40] Feinberg DA, Moeller S, Smith SM, Auerbach E, Ramanna S, Glasser MF, et al. Multiplexed echo planar imaging for sub-second whole brain FMRI and fast diffusion imagingValdes-Sosa PA, editor. PLoS One 2010 Dec 20;5(12):e15710.
[41] Xu J, Moeller S, Auerbach EJ, Strupp J, Smith SM, Feinberg DA, et al. Evaluation of slice accelerations using multiband echo planar imaging at 3T. Neuroimage 2013 Dec;83:991–1001.
[42] Jenkinson M, Beckmann CF, Behrens TEJ, Woolrich MW, Smith SM. Fsl. Neuroimage 2012;62(2):782–90.
[43] Jenkinson M, Bannister P, Brady M, Smith S. Improved optimization for the robust and accurate linear registration and motion correction of brain images. Neuroimage 2002 Oct;17(2):825–41.
[44] Salimi-Khorshidi G, Douaud G, Beckmann CF, Glasser MF, Griffanti L, Smith SM. Automatic denoising of functional MRI data: combining independent component analysis and hierarchical fusion of classifiers. Neuroimage 2014 Apr;90:449–68.
[45] Griffanti L, Salimi-Khorshidi G, Beckmann CF, Auerbach EJ, Douaud G, Sexton CE, et al. ICA-based artefact removal and accelerated fMRI acquisition for improved resting state network imaging. Neuroimage 2014 Jul;95:232–47.

[46] Beckmann CF, Jenkinson M, Smith SM. General multilevel linear modeling for group analysis in FMRI. Neuroimage 2003 Oct;20(2):1052–63.
[47] Fan L, Li H, Zhuo J, Zhang Y, Wang J, Chen L, et al. The human brainnetome Atlas: a new brain Atlas based on connectional Architecture. Cerebr Cortex 2016 Aug;26 (8):3508–26.
[48] Ni Z, Gunraj C, Nelson AJ, Yeh IJ, Castillo G, Hoque T, et al. Two phases of interhemispheric inhibition between motor related cortical areas and the primary motor cortex in human. Cerebr Cortex 2009 Jul 1;19(7):1654–65.
[49] Irlbacher K, Brocke J, Mechow Jv, Brandt SA. Effects of GABAA and GABAB agonists on interhemispheric inhibition in man. Clin Neurophysiol 2007 Feb;118 (2):308–16.
[50] Schwab BC, König P, Engel AK. Spike-timing-dependent plasticity can account for connectivity aftereffects of dual-site transcranial alternating current stimulation. Neuroimage 2021;237(March):118179.
[51] Heise KF, Albouy G, Dolfen N, Peeters R, Mantini D, Swinnen SP. Induced zero-phase synchronization as a potential neural code for optimized visuomotor integration. Brain Stimulat 2025 Mar;S1935861X25000762.
[52] Jenkins IH, Jahanshahi M, Jueptner M, Passingham RE, Brooks DJ. Self-initiated versus externally triggered movements. II. The effect of movement predictability on regional cerebral blood flow. Brain 2000;123(6):1216–28.
[53] Lu MK, Arai N, Tsai CH, Ziemann U. Movement related cortical potentials of cued versus self-initiated movements: double dissociated modulation by dorsal premotor cortex versus supplementary motor area rTMS. Hum Brain Mapp 2012;33(4): 824–39.
[54] Mushiake H, Inase M, Tanji J. Neuronal activity in the primate premotor, supplementary, and precentral motor cortex during visually guided and internally determined sequential movements. J Neurophysiol 1991;66(3):705–18.
[55] Callaert DV, Vercauteren K, Peeters R, Tam F, Graham S, Swinnen SP, et al. Hemispheric asymmetries of motor versus nonmotor processes during (visuo)motor control. Hum Brain Mapp 2011 Aug;32(8):1311–29.
[56] Heise KF, Monteiro TS, Leunissen I, Mantini D, Swinnen SP. Distinct online and offline effects of alpha and beta transcranial alternating current stimulation (tACS) on continuous bimanual performance and task-set switching. Sci Rep 2019 Dec 1;9 (1).
[57] Lafleur LP, Klees-Themens G, Chouinard-Leclaire C, Larochelle-Brunet F, Tremblay S, Lepage JF, et al. Neurophysiological aftereffects of 10 Hz and 20 Hz transcranial alternating current stimulation over bilateral sensorimotor cortex. Brain Res 2020 Jan;1727:146542.
[58] Rostami M, Lee A, Frazer AK, Akalu Y, Siddique U, Pearce AJ, et al. Determining the effects of transcranial alternating current stimulation on corticomotor excitability and motor performance: a sham-controlled comparison of four frequencies. Neuroscience 2025 Mar;568:12–26.
[59] Hiromitsu K, Asai T, Kadota H, Imaizumi S, Kamata M, Imamizu H. Immediate modulation of the blood oxygenation level-dependent signals by dual-site transcranial alternating current stimulation propagates across the whole brain [internet] [cited 2024 Sep 13]. Available from: http://biorxiv.org/lookup/doi/10.1101/2024.09.03.610912; 2024.
[60] Vosskuhl J, Huster RJ, Herrmann CS. BOLD signal effects of transcranial alternating current stimulation (tACS) in the alpha range: a concurrent tACS–fMRI study. Neuroimage 2016 Oct;140:118–25.
[61] Vieira PG, Krause MR, Laamerad P, Pack CC. Brain stimulation preferentially influences long-range projections in primates [internet]. 2025. http://biorxiv.org/lookup/doi/10.1101/2025.02.19.639189. [Accessed 4 March 2025].
[62] Wischnewski M, Engelhardt M, Salehinejad MA, Schutter DJLG, Kuo MF, Nitsche MA. NMDA receptor-mediated motor cortex plasticity after 20 Hz transcranial alternating current stimulation. Cerebr Cortex 2019 Jul 5;29(7): 2924–31.
[63] Kasten Dowsett. Herrmann. Sustained aftereffect of α-tACS lasts up to 70 min after stimulation. Front Hum Neurosci 2016;10.
[64] Zaehle T, Rach S, Herrmann CS. Transcranial alternating current stimulation enhances individual alpha activity in human EEGAleman A, editor. PLoS One 2010 Nov 1;5(11):e13766.
[65] Helfrich RF, Schneider TR, Rach S, Trautmann-Lengsfeld SA, Engel AK, Herrmann CS. Entrainment of brain oscillations by transcranial alternating current stimulation. Curr Biol 2014 Feb;24(3):333–9.
[66] Neuling T., Rach S., Herrmann C.S. Orchestrating neuronal networks: sustained after-effects of transcranial alternating current stimulation depend upon brain states. Front Hum Neurosci [Internet] 2013;7:1-12. [cited 2025 May 22]. Available from: http://journal.frontiersin.org/article/10.3389/fnhum.2013.00161/abstract.
[67] Gann, Schwab, Stagg. Behavioural and group fMRI data from young healthy participants engaged in a bimanual coordination task with concurrent dual-site beta M1 tACS [internet]. Available from: https://doi.org/10.60964/bndu-mw4b-t114.